Supporting Information

Crystalline Medium-Bandgap Light-harvesting Donor Material Based on *β*-Naphthalene Asymmetric-modified Benzodithiophene Moiety towards Efficient Polymer Solar Cells

Yonghai Li,[†] Deyu Liu,[†,‖] Junyi Wang,[†,‖] Zhi-Guo Zhang,[§] Yongfang Li,[§] Yanfang Liu,[†] Tingting Zhu,[‡] Xichang Bao,*[,†] Mingliang Sun[‡] and Renqiang Yang*[,†]

[†] CAS Key Laboratory of Bio-based Materials, Qingdao Institute of Bioenergy and Bioprocess Technology, Chinese Academy of Sciences, Qingdao 266101, China.

[‡] Institute of Material Science and Engineering, Ocean University of China, Qingdao 266100, China.

[§] Beijing National Laboratory for Molecular Sciences, CAS Key Laboratory of Organic Solids, Institute of Chemistry, Chinese Academy of Sciences, Beijing 100190, China.

[‖] University of Chinese Academy of Sciences, Beijing 100049, China.

1. Materials and Characterization Techniques

Acceptor materials $PC_{71}BM$ and ITIC are purchased from Solarmer Materials Inc. All solvents and reagents were purchased from Alfa Aesar, Sigma-Aldrich, which were utilized directly unless stated otherwise.

^{1}H NMR and ^{13}C NMR spectra were recorded on Bruker AVANCE III 600 MHz spectrometer at 298 K. TGA measurement was performed using a SDT Q600 V20.9 Build 20 at a heating rate of 10 ^{o}C min^{-1} under a nitrogen atmosphere. The absorption spectra were recorded using a Hitachi U-4100 UV-Vis scanning spectrophotometer. Photoluminescence spectra were measured using a Fluoromax-4 fluorescence spectrometer. Cyclic voltammetry (CV) measurements were performed on a CHI660D electrochemical workstation, equipped with a three-electrode cell consisting of a platinum working electrode, a saturated calomel electrode (SCE) as reference electrode and a platinum wire counter electrode. CV measurements were carried out in anhydrous acetonitrile containing 0.1 M *n*-Bu_4NPF_6 as a supporting electrolyte under an argon atmosphere at a scan rate of 100 mV s^{-1}. Thin films were deposited from *o*-DCB solution onto the working electrodes. Grazing incidence wide-angle X-ray scattering (GIWAXS) patterns were acquired by beamline BL16B1 (Shanghai Synchrotron Radiation Facility). Gel permeation chromatography (GPC) was performed with trichlorobenzene (TCB) as eluent at 150 °C and polystyrene was used as the standard.

2. Device Fabrication and Evaluations

The PSCs devices were fabricated with a configuration of ITO/PEDOT:PSS/*asy*-PBDBTN:$PC_{71}BM$ or ITIC/PDINO/Al. The patterned ITO glass (sheet resistance = 15 Ω/square) was pre-cleaned in an ultrasonic bath of acetone and isopropyl alcohol and treated in an ultraviolet-ozone chamber (PREEN II-862) for 6 min. Then a thin layer (about 30 nm) of PEDOT:PSS was spin-coated onto the ITO glass at 4000 rpm and

baked at 150 °C for 15 min. Solutions of polymer/$PC_{71}BM$ in *o*-DCB (25 mg/mL) or polymer/ITIC in chlorobenzene (20 mg/mL) were stirred overnight and warmed to 50 °C for 30 mins before spin-coating on the PEDOT:PSS layer to form the active layer about 100-120 nm. The thickness of the active layer was measured using a Veeco Dektak 150 profilometer. PDINO in methanol (1 mg/mL) was spin-coated at 3000 rpm to form electron-transfer layer. Finally, Al (100 nm) metal electrode was thermal evaporated under about 4×10^{-4} Pa and the device area was 0.1 cm^2 defined by shadow mask.

The current density–voltage (*J–V*) characteristics were recorded with a Keithley 2400 source measurement unit under simulated 100 mW cm^{-2} irradiation from a Newport solar simulator. The external quantum efficiencies (EQEs) were analysed using a certified Newport incident photon conversion efficiency (IPCE) measurement system. The hole mobility and electron mobility were measured by space-charge-limited current (SCLC) method with a device configuration of ITO/PEDOT:PSS/active layer/MoO_3/Al and ITO/ZnO/active layer/PFN/Al structure, respectively. The SCLC is described by the Mott–Gurney law:

$$J = \frac{9}{8}\varepsilon_0\varepsilon_r\mu\frac{(V_a - V_{bi})^2}{d^3} \qquad \text{(S1)}$$

In equation (S1), J is current density, ε_0 is permittivity of vacuum, ε_r is relative permittivity of the transport medium, μ is mobility, V_a is applied voltage, V_{bi} is built-in voltage, and d is the thickness of the active film.

3. Synthetic Route

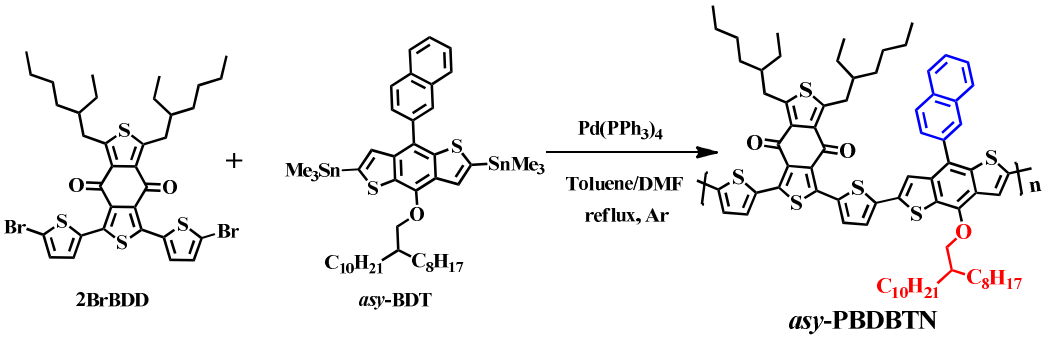

Scheme S1. Synthetic route of polymer *asy*-PBDBTN

Monomer 2BrBDD was synthesized according to previous report.[S1] Monomer *asy*-BDT was obtained in our previous work.[S2]

Synthesis of asy-PBDBTN: 2BrBDD (0.12 mmol, 92.0 mg), *asy*-BDT (0.12 mmol, 112.6 mg) were dissolved in the mixture of dry toluene (8.0 mL) and DMF (0.50 mL). The solution was purged with Ar for 30 min., and then $Pd(PPh_3)_4$ (0.0086 mmol, 10.0 mg) was added. The reaction was refluxed for 20 hrs. After cooling to room temperature, the resulting mixture was poured into methanol under stirring. The precipitates were filtered off and subjected to Soxhlet extraction successively with methanol, acetone and hexane for the removal of remaining monomers, oligomers and catalytic impurities. The polymer was collected using chloroform as the eluent. Solvent was removed and the residue was re-dissolved in chloroform and precipitated against methanol. The precipitates were filtered, washed with methanol, and dried under vacuum at 50 ^{o}C overnight to obtain *asy*-PBDBTN as purple solids (139 mg, yield: 94.5%). M_n (GPC, TCB, 150 ^{o}C) = 40.6 kD, PDI = 2.7. Decomposition temperature (N_2, 5% weight loss): 322 ^{o}C.

4. TGA analysis

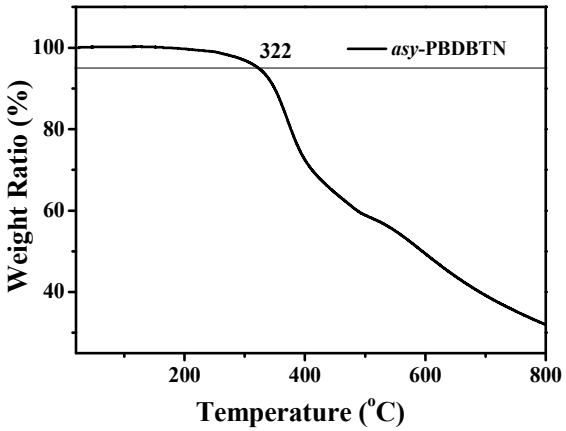

Figure S1. The TGA curve of polymer *asy*-PBDBTN at a heating rate of 10 ^{o}C min^{-1} under nitrogen atmosphere.

5. DFT calculations

Table S1. HOMO and optimal ω values for the molecular system studied in this work

Isolated molecular	
ω (bohr−1)	HOMO (eV)
0.05	-5.48
0.10	-5.97
0.12	-6.15
0.15	-6.39
0.20	-6.73
	-5.41 Experimental

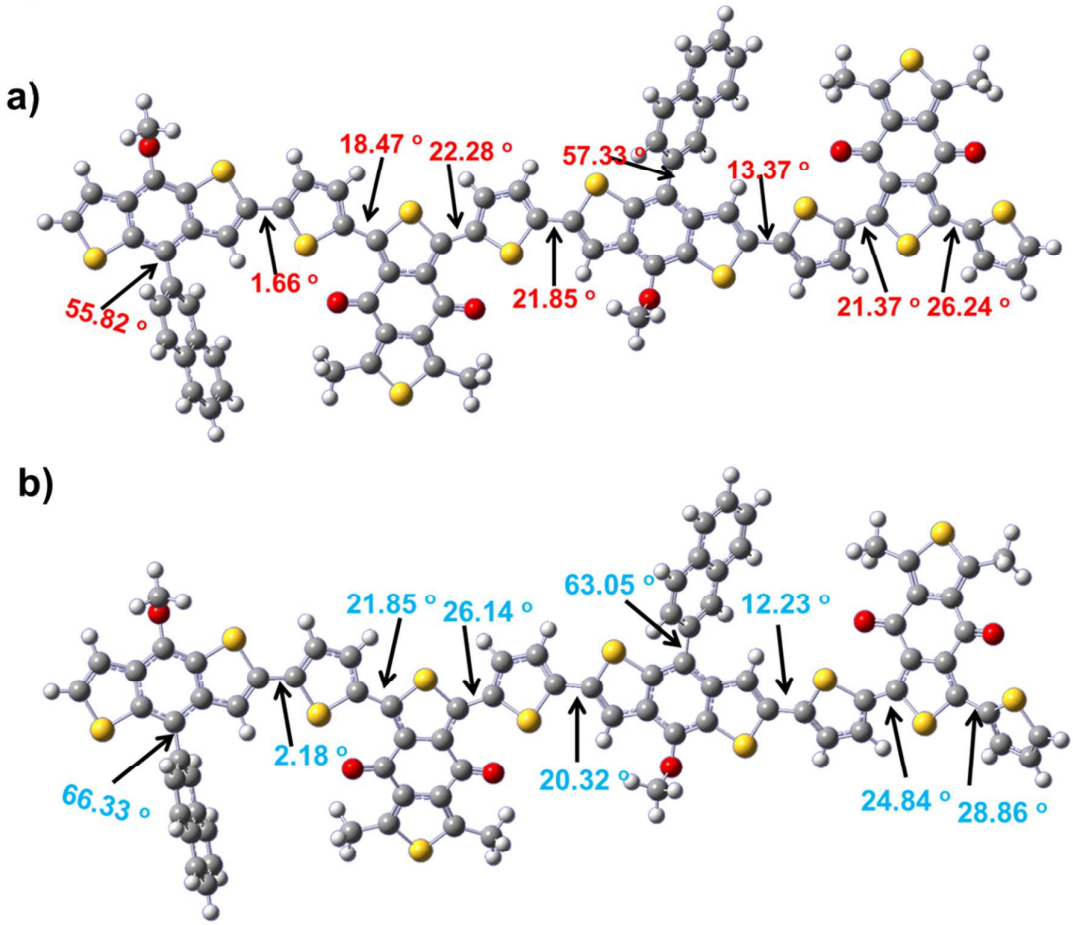

Figure S2. The dihedral angles of polymer *asy*-PBDBTN (dimers of repeat unit) based on DFT calculations at ωB97XD functional with different ω values (ω=0.2 for figure a, ω=0.05 for figure b).

6. Basic Properties

Table S2. Decomposition temperature, molecular weight, optical properties and energy levels of the polymer

Polymer	Thermal Stability	Molecular Weight		Absorption		Electrochemistry		
	T_d[a]	M_n (kDa)	PDI	$\lambda_{max,sol}$ (nm)	$\lambda_{max,film}$ (nm)	E_g^{opt} (eV)[b]	HOMO (eV)	LUMO (eV)
asy-PBDBTN	322	40.6	2.7	623	621	1.83	-5.41	-3.58

[a] Measured under N_2 atmosphere; [b] Calculated based on the onset of thin film absorption spectra.

7. Absorption Spectra

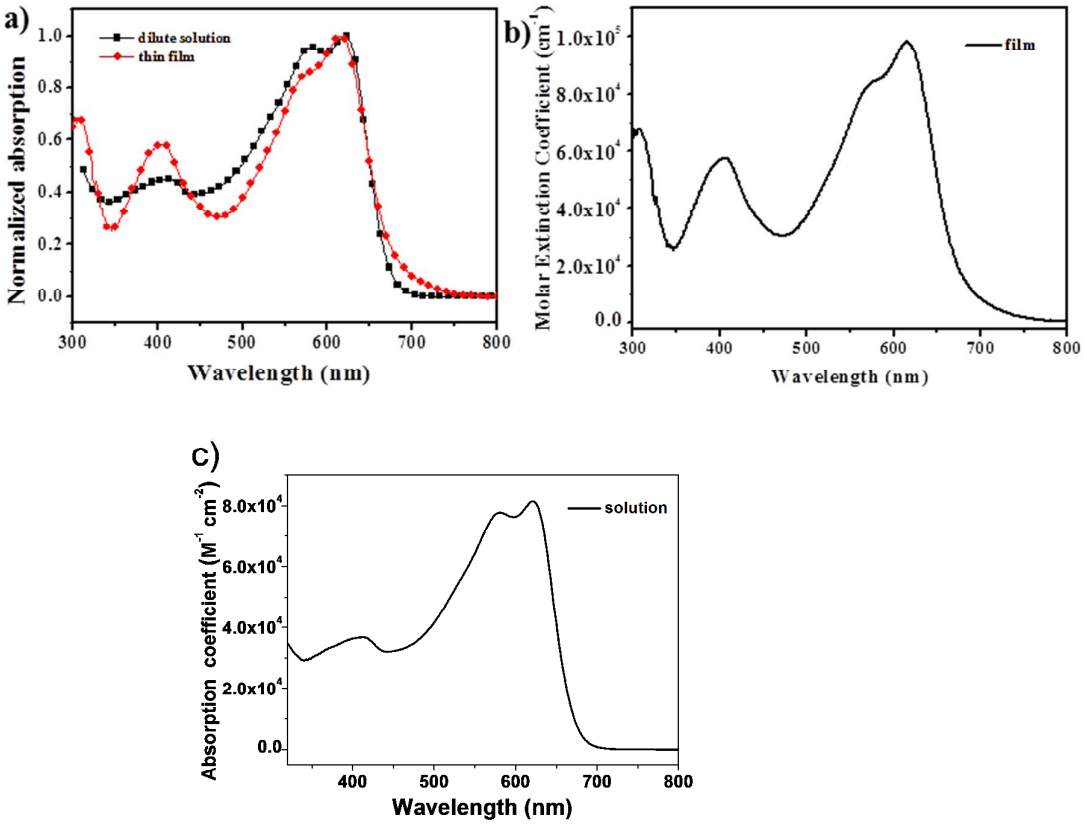

Figure S3. (a) Uv-Vis absorption spectra of polymer *asy*-PBDBTN in dilute solution (*o*-DCB, 10^{-5} M) and as thin film; (b) the molar extinction coefficient of *asy*-PBDBTN as thin film; (c) the molar extinction coefficient of *asy*-PBDBTN in dilute solution (o-DCB, 10^{-5} M).

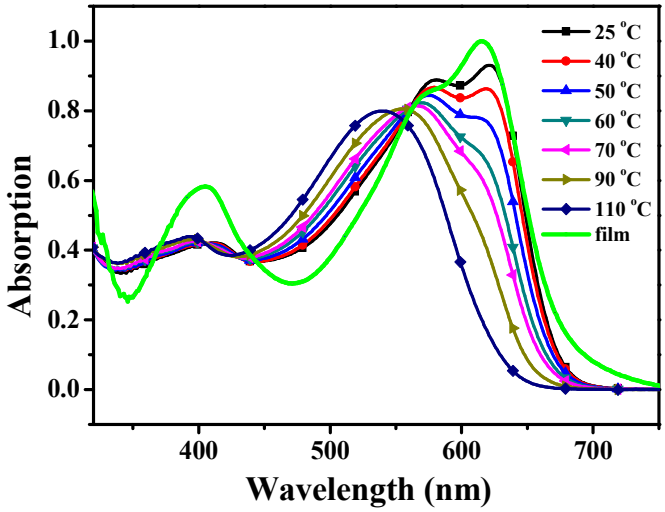

Figure S4. Uv-Vis spectra of polymer *asy*-PBDBTN in dilute solution (*o*-DCB, 10^{-5} M) with temperature dependence.

8. Electrochemical Property

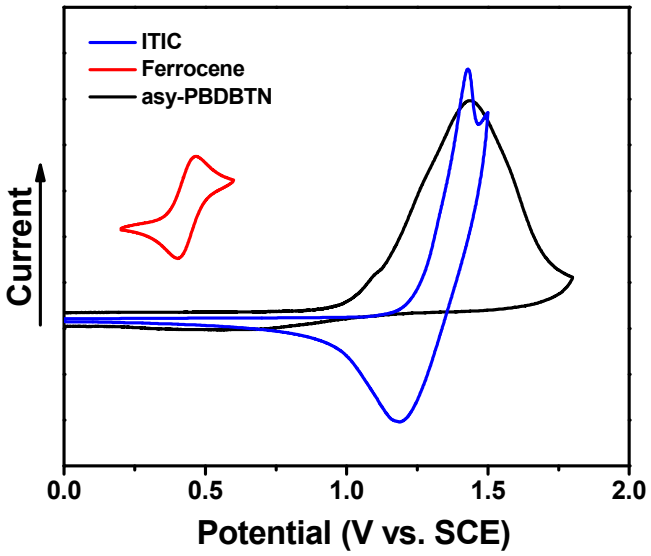

Figure S5. Cyclic voltammograms of polymer *asy*-PBDBTN and ITIC on Pt electrodes in 0.1 M Bu_4NPF_6-CH_3CN solution at a scan rate of 100 mV s^{-1}.

9. Photovoltaic Performance

Table S3 Device parameters of PSCs under optimal weight ratio

Active layer	*w/w*	Thickness (nm)	DIO (%)	V_{OC}[a] (V)	J_{SC}[a] (mA cm^{-2})	FF[a]	PCE[a] (%)
asy-PBDBTN/ $PC_{71}BM$	1:0.8	110±5		0.948 (0.943±0.004)	11.33 (11.02±0.28)	0.612 (0.599±0.010)	6.57 (6.28±0.23)
	1:1	115±5		0.930 (0.921±0.006)	12.65 (12.38±0.23)	0.692 (0.681±0.013)	8.14 (7.90±0.19)
	1:1.5	115±5		0.916 (0.908±0.009)	11.93 (11.71±0.21)	0.712 (0.701±0.011)	7.78 (7.58±0.20)
	1:1	115±5	1.0	0.924 (0.914±0.010)	13.30 (12.97±0.31)	0.708 (0.699±0.007)	8.70 (8.54±0.24)
	1:1	115±5	1.5	0.893 (0.884±0.007)	13.98 (13.77±0.19)	0.711 (0.702±0.009)	8.88 (8.59±0.27)
	1:1	115±5	2.0	0.889 (0.881±0.005)	12.77 (12.53±0.16)	0.699 (0.685±0.012)	7.94 (7.74±0.18)
asy-PBDBTN/ ITIC	1:0.8	115±5		0.941 (0.929±0.010)	14.85 (14.58±0.19)	0.602 (0.595±0.008)	8.41 (8.21±0.16)
	1:1	120±5		0.951 (0.940±0.011)	15.69 (15.44±0.26)	0.640 (0.633±0.006)	9.55 (9.28±0.22)
	1:1.5	110±5		0.948 (0.940±0.009)	15.26 (15.05±0.17)	0.625 (0.621±0.005)	9.04 (8.82±0.20)
	1:1	120±5	0.25	0.950 (0.939±0.010)	16.22 (15.99±0.21)	0.641 (0.633±0.009)	9.88 (9.63±0.25)
	1:1	120±5	0.5	0.947 (0.941±0.007)	16.42 (16.08±0.33)	0.650 (0.638±0.011)	10.11 (9.85±0.21)

1:1	120±5	0.75	0.944 (0.933±0.009)	16.18 (15.92±0.27)	0.643 (0.631±0.010)	9.82 (9.56±0.23)
1:1[b]	120±5	0.5	0.942 (0.930±0.009)	16.81 (16.48±0.30)	0.663 (0.654±0.011)	10.50 (10.22±0.20)

[a] Data were provided in optimal (statistical) results based on 34 devices; [b] The blend films of *asy*-PBDBTN/ITIC (1:1, 0.5% DIO, the last line) were thermal annealed at 150 °C for 10 mins.

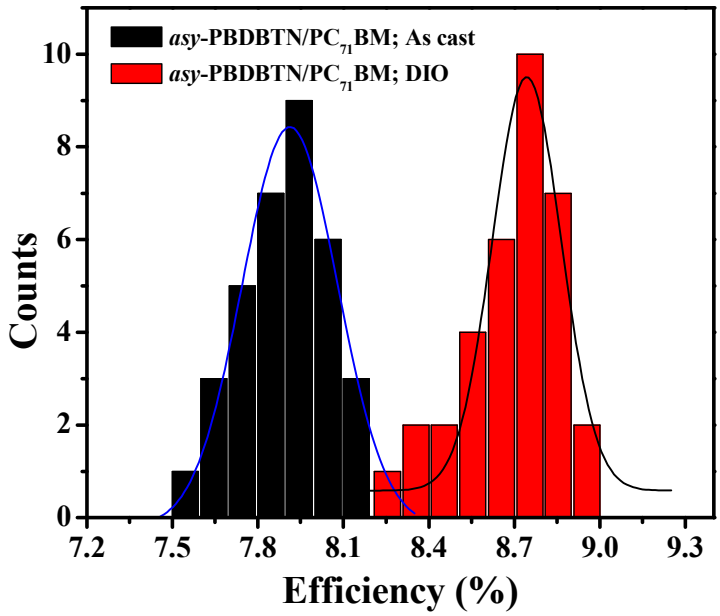

Figure S6. Statistical histogram of PCEs of PSCs based on *asy*-PBDBTN:$PC_{71}BM$ (*w*/*w*=1:1) before and after optimization. (34 devices for each case)

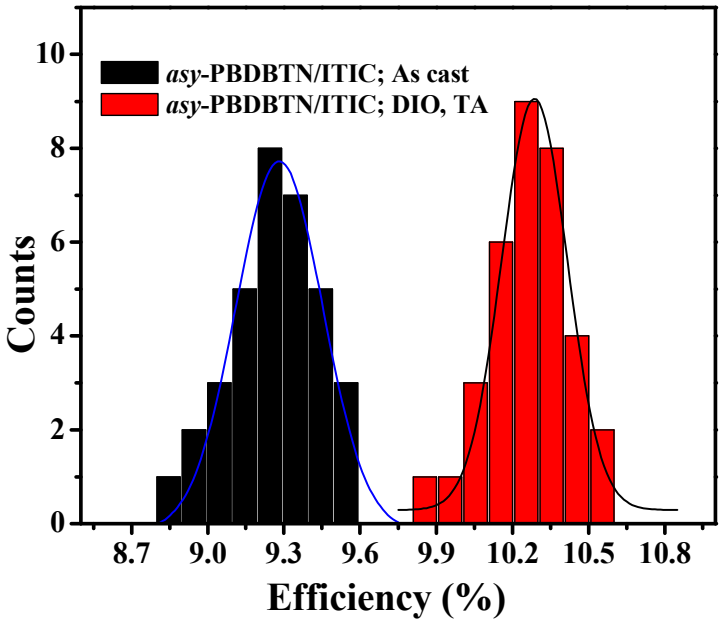

Figure S7. Statistical histogram of PCEs of PSCs based on *asy*-PBDBTN:ITIC (*w/w*=1:1) before and after optimization (TA=thermal annealing). (34 devices for each case)

10. SCLC measurements

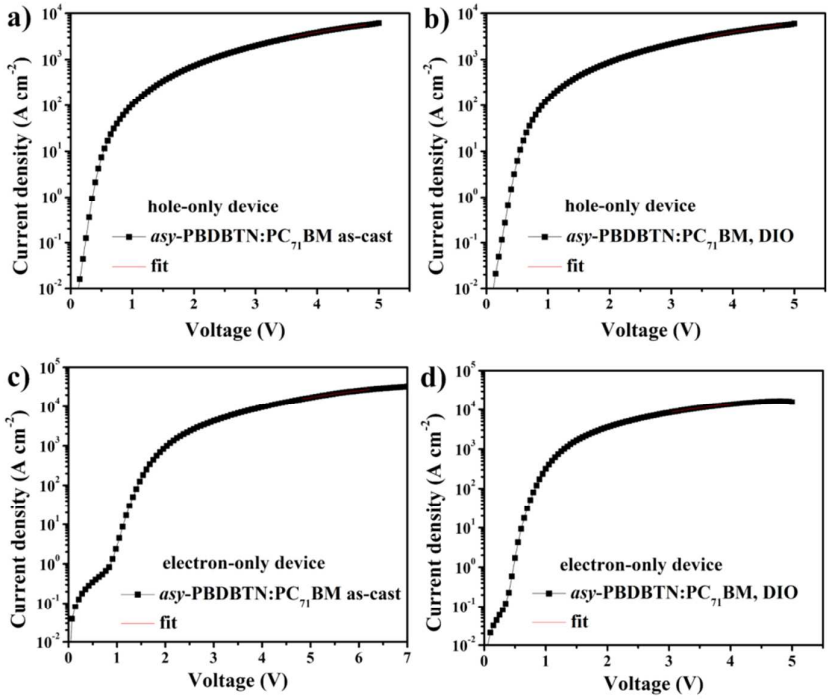

Figure S8. SCLC curves for *asy*-PBDBTN:$PC_{71}BM$ based hole-only (a, b) and electron-only (c, d) devices under different treatments.

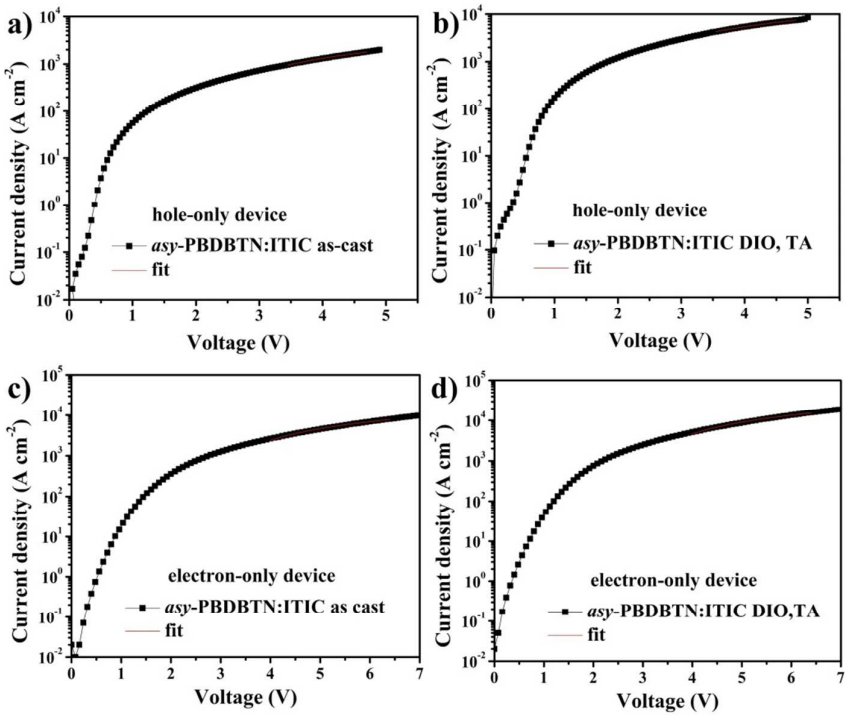

Figure S9. SCLC curves for *asy*-PBDBTN:ITIC based hole-only (a, b) and electron-only (c, d) devices under different treatments (TA=thermal annealing).

11. Integrated current densities based on EQE measurements

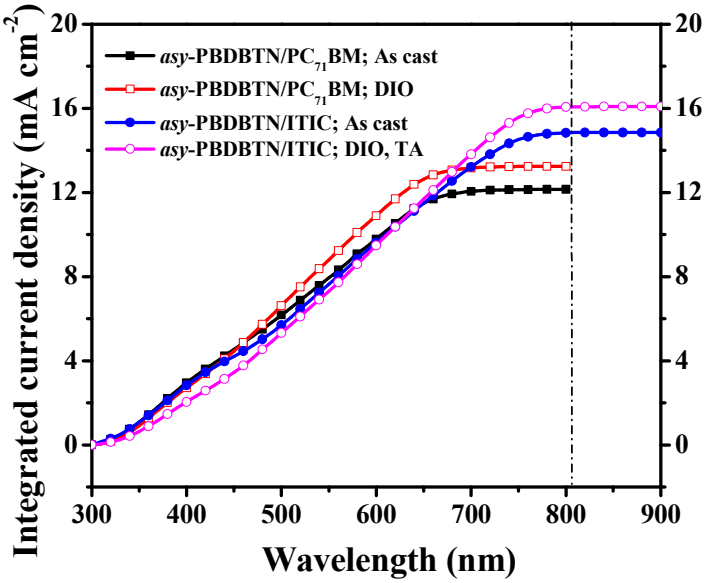

Figure S10. The integrated current densities of four PSCs based on EQE measurements under the respective optimal conditions (TA=thermal annealing).

12. AFM and TEM measurements

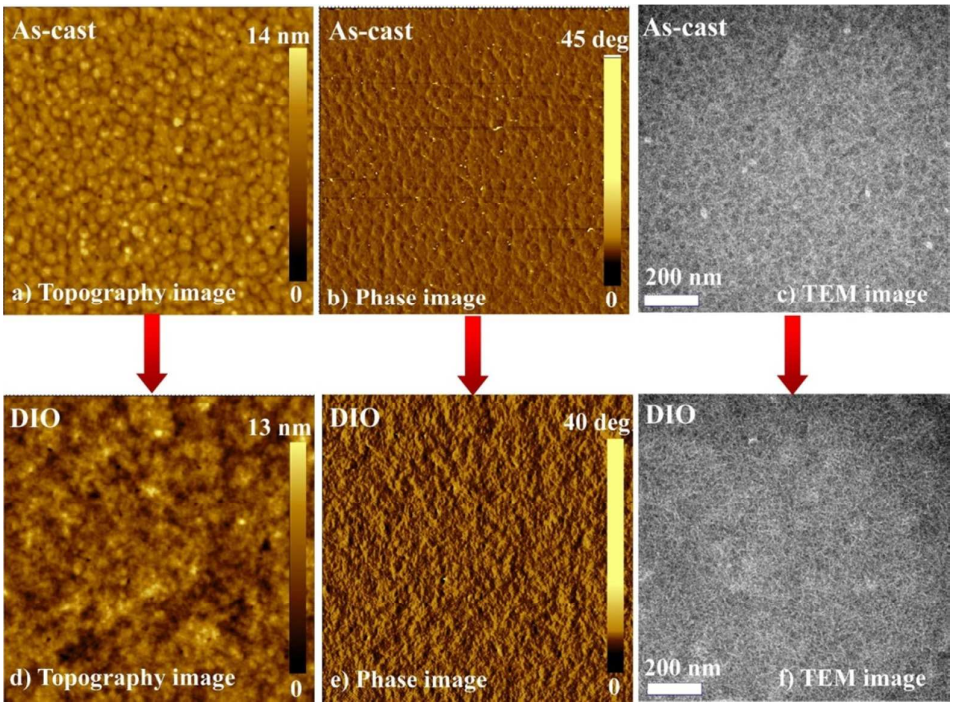

Figure S11. AFM topography (a, d) and phase images (b, e, 2.5 μm × 2.5 μm) and TEM images (c, f) of *asy*-PBDBTN:$PC_{71}BM$ blend films (*w*/*w*=1:1) under different conditions .

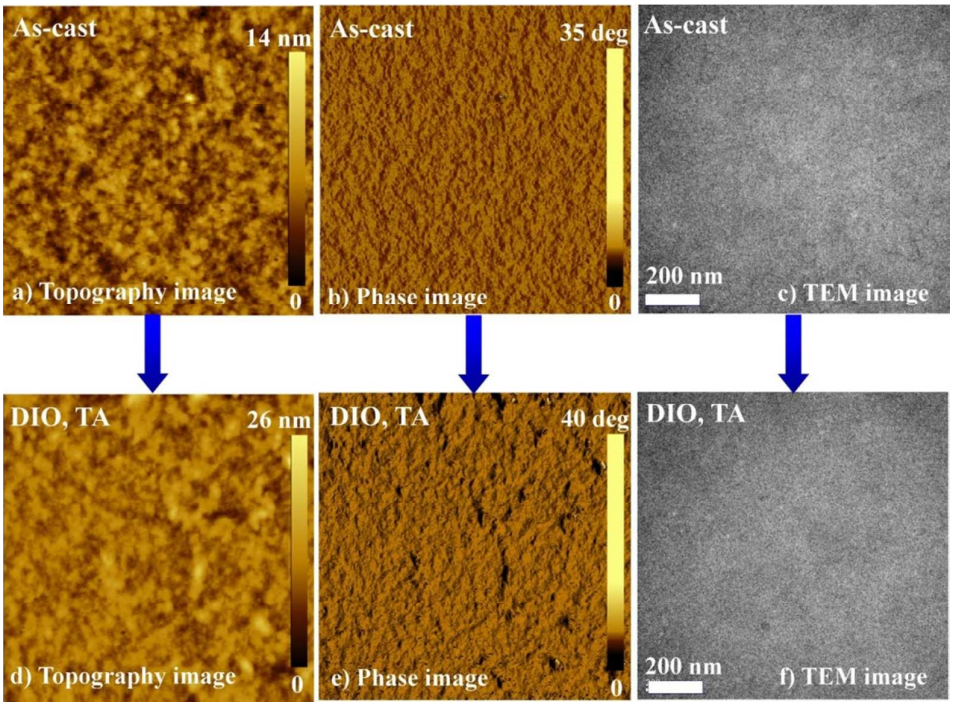

Figure S12. AFM topography (a, d) and phase images (b, e, 2.5 μm × 2.5 μm) and TEM images (c, f) of *asy*-PBDBTN:ITIC blend films (*w*/*w*=1:1) under different conditions (TA=thermal annealing).

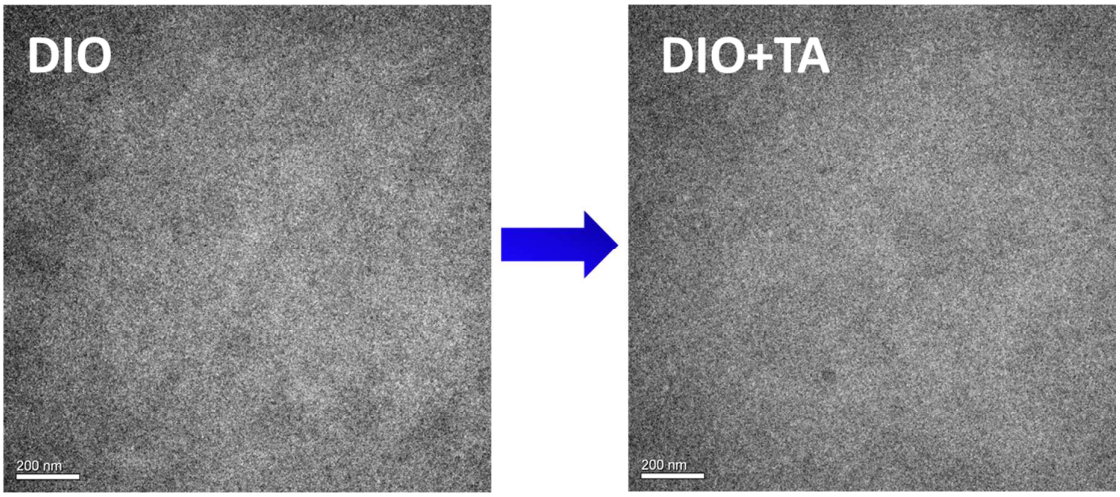

Figure S13. TEM images of *asy*-PBDBTN:ITIC blend films (*w/w*=1:1, 0.5% DIO) before and after thermal annealing (TA=thermal annealing).

13. The Structure Data from GIWAXS Measurements

Table S4 The lamellar distances and the π-π-stacking distances of the films

Films	Lamellar distances (100)		π-π-stacking distances (010)	
	q ($Å^{-1}$)	*d* (Å)	q ($Å^{-1}$)	*d* (Å)
asy-PBDBTN	0.3755	16.76	1.6924	3.71
asy-PBDBTN:$PC_{71}BM$	0.3693	17.01	-	-
asy-PBDBTN:$PC_{71}BM$, DIO	0.3313	18.96	1.7412	3.61
asy-PBDBTN:ITIC	0.3515	17.87	1.7031	3.69
asy-PBDBTN:ITIC, DIO	0.3501	17.94	1.6972	3.70
asy-PBDBTN:ITIC, DIO+TA [a]	0.3314 0.4312	18.96 14.57	1.7212 1.5744	3.65 3.98

[a] TA=thermal annealing

14. The ^{1}H NMR spectra of *asy*-PBDBTN

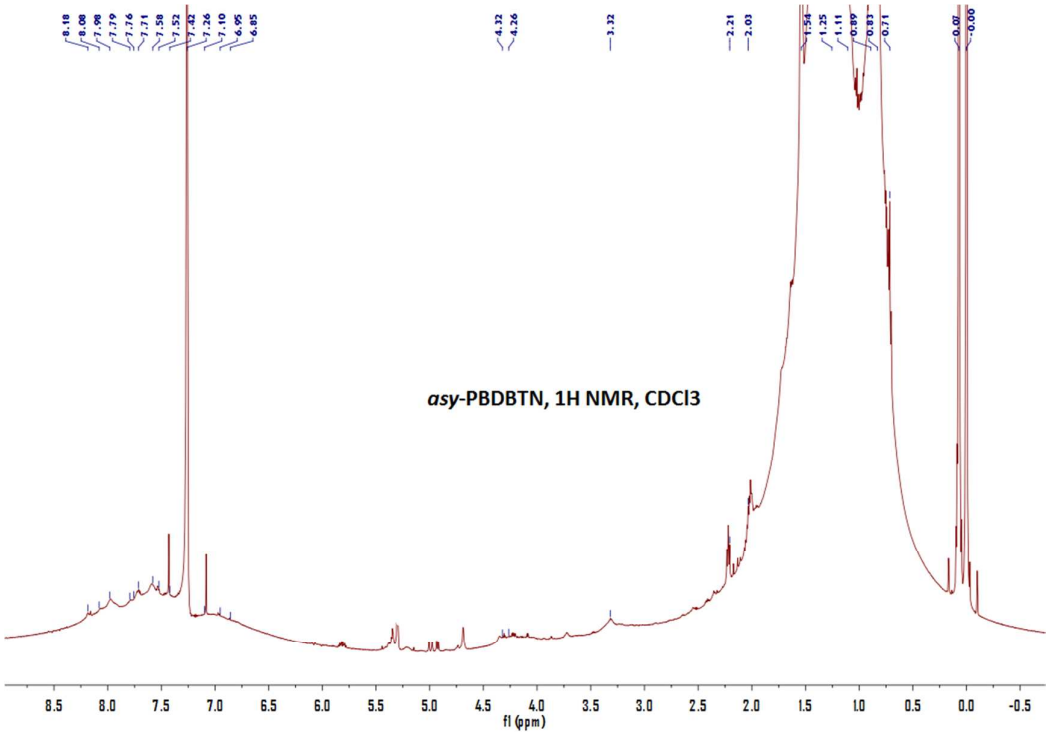

References:

[S1] Qian, D.; Ye, L.; Zhang, M.; Liang, Y.; Li, L.; Huang, Y.; Guo, X.; Zhang, S.; Tan, Z.; Hou, J., *Macromolecules* **2012**, *45*, 9611.

[S2] Liu, D.; Gu, C.; Wang, J.; Zhu, D.; Li, Y.; Bao, X.; Yang, R., *J. Mater. Chem. A* **2017,** *5,* 9141.